

Teorijska hemija / Theoretical Chemistry

Influence of protein environment on redox properties of cofactors: Redox potentials of artificial cytochrome b

Dragan M. Popović, Ivan O. Juranić

*Institute for Chemistry, Technology and Metallurgy, Department of Chemistry, University of Belgrade,
Njegoševa 12, 11000 Belgrade, Serbia
(dpopovic@chem.bg.ac.rs, ijuranic@chem.bg.ac.rs)*

Model building from scratch with advanced modeling techniques is used to generate the atomic coordinates of 25 synthetic cytochrome b proteins. Protonation pattern and redox potentials of heme are evaluated from electrostatic energies. The computed redox potentials generally agree well with experimental measurements. The factors of protein environment determining the shift in the redox potentials are elucidated and open up new avenues of protein design.

Introduction

Proteins that have tailored structural and functional properties are needed as central components of biosensors in bioelectronics and bio-nanotechnology. Such novel proteins can be designed by site directed mutagenesis starting from native proteins, by screening large libraries of polypeptides to find a protein with desired properties or by chemical synthesis with libraries of short linear and cyclic polypeptides using a modular building principle.¹ Much effort was devoted to develop the techniques to synthesize polypeptides from scratch and to assemble them to model artificial proteins.² One focus was to study the interaction of polypeptide environment with heme as cofactor.³

The architecture of two pairs of antiparallel α -helices covalently attached to a cyclic peptide is a building principle to generate synthetic proteins with a four-helix bundle structure.^{2c} This method was successfully applied to construct models of cytochrome b (cyt b) with one or two hemes.⁴ The synthetic cyt b analogs were electronically active when bound to a gold surface⁴ and exhibited light-induced electron transfer when bound to a metallo-protein.⁵

Rational design of artificial proteins requires knowledge about structure. So far only for one artificial four-helix bundle protein an NMR deduced structure is available.^{6a} But recently, atomic coordinates were generated from scratch by advanced modeling techniques^{6b} for a synthetic cyt b with two hemes^{4a} that can serve as model for the cyt b subunit of the membrane spanning photosynthetic cytochrome b_6f and the mitochondrial cytochrome bc_1 protein complexes. In molecular dynamics (MD) simulations the synthetic cyt b proteins exhibited root mean square deviations (RMSD) from the initial structure, which were as small as values typically obtained by using the atomic coordinates of a crystal structure, demonstrating the robustness of the model structures.^{6b,7}

Based on the model structure the redox potentials of the hemes were computed by evaluating the electrostatic energy difference between oxidized and reduced states averaged over all possible charge states of titratable residues by solving the Poisson-Boltzmann equation (PBE). The computational procedure and the charge models that we used were validated by considering also the cyt b subunit from the crystal structure of the native cytochrome bc_1 complex,^{7b} where measured and calculated redox potentials of the two hemes agree to within 20 mV. The generated model structure of the synthetic cyt b was validated by comparing computed and measured redox potentials of the two hemes yielding deviations of less than 15 mV.^{6b}

The success to model the structure of a synthetic protein-cofactor complex opens the possibility to investigate how the protein environment tunes the redox potential of cofactors. A suitable model system is the synthetic cyt b with a single heme as cofactor, where the redox potential was measured for 400 different mutants.^{4d} Cyt b consists of two pairs of identical helices A and B, which are covalently linked to a cyclic decapeptide serving as template to form an antiparallel four-helix bundle. Two histidines that are axial ligands of heme are located in the helix pair of type B. The variation of these amino acids was restricted to hydrophobic side chains of different sizes, two polar (Tyr, Gln) and the basic residue Arg.

Results and discussion

The atomic coordinates of 25 synthetic cyt b were generated in the similar fashion as described previously.^{6b} The sequences (listed in Figure 2) were chosen to cover the whole range of measured redox potentials (−89 mV to −148 mV) of 400 artificial cyt b that were synthesized.^{4c} We also considered sequence 24 and 25, where redox potential could not be measured, since it was outside of range of the used redox indicator. A larger portion of mutants focuses on the interface between helix pairs A₁/B₁ and A₂/B₂, where $\alpha_4\alpha_{11}$ and $\beta_5\beta_{12}$ are varied such that with the exception of Arg mostly hydrophobic residues come together (see helical wheel projection of four-helix bundle, Figure 1a). Two possible modes to place the heme in the pocket of the four-helix bundle were considered. (i) The propionates of heme are oriented towards the template, (ii) or they are oriented towards the open end of the four-helix bundle. We generated all 25 structures with heme conformation (i). For the sequences 1, 4, 8, 14, 15, 16, 23, we also generated structures with heme conformation (ii). The structure of the synthetic cyt b with sequence 17 and heme conformation (i) is shown in Figure 1b. The free energy difference of the two heme conformations was computed from the electrostatic energies by solving the PBE averaged over the protonation states of all titratable groups including non-electrostatic conformation energy from CHARMM⁸ and a surface energy term yielding −1.9 (−1.0, +0.4, +5.2, −7.0) kcal/mol for structures 4 (8, 14, 15, 23) favoring heme conformation (i).

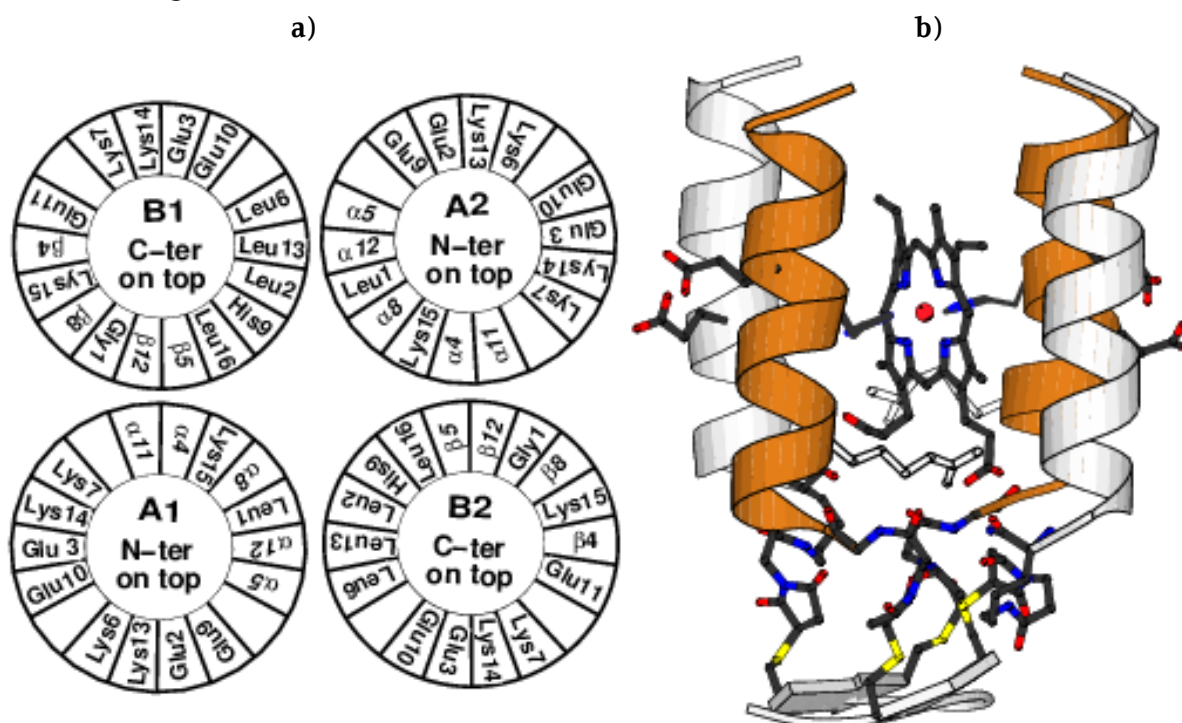


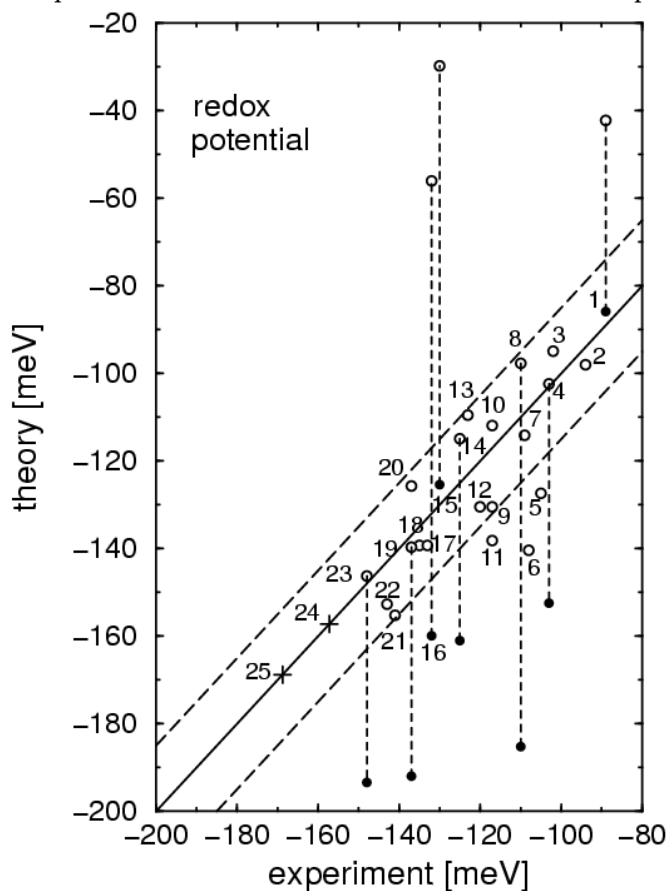
Figure 1. a) Topology of the four-helix bundle in helical wheel projection. The representation is useful to locate the residues on the surface, in the interfacial region or in the interior of the four-helix bundle. The sequences are LEE $\alpha_4\alpha_5$ KK α_8 EE $\alpha_{11}\alpha_{12}$ KKK for helix A and GLE $\beta_4\beta_5$ LK β_8 HEE β_{12} LKKL for helix B. Greek letters denote positions with variable amino acids. The 25 variable sequence parts that were considered are given in caption of Figure 2.

b) Structure of the synthetic cyt b with sequence 17. The helices A and B are represented as light gray and dark orange rubber bands, respectively. The β -turn structure of the cyclic decapeptide serving as template is shown by a pair of gray arrows. The ϵ -amino group of the C-terminal Lys15 of helices A and the N-terminus of helices B are coupled with the 3-maleimidopropionic acids. Helices A are bound to the template with the C-terminal Lys15 side chain, while helices B are bound with the backbone of the N-terminal Gly1 by coupling of the so created maleinodopropionyl moiety of the helices A and B to the cystein side chains of the cyclic decapeptide. Besides the heme and the axially coordinated histidines the pairs of glutamates E9(A₂)/E10(B₁) and E9(A₁)/E10(B₂) as well as the arginines R5(B₁) and R5(B₂) are displayed in atomic details.

The protonation pattern of titratable residues and the redox potentials of the 25 modeled synthetic cyt b were calculated from the solution of the PBE. Lys and Glu are generally charged except for the two pairs of glutamates E9(A₂)/E10(B₁) and E9(A₁)/E10(B₂) that are partially protonated due to their mutual proximity and partially hydrophobic neighborhood. Arg at position α_5 in helix A₂ (sequence 1, 15) is

fully protonated and forms a salt bridge with the corresponding pair of glutamates E9(A₂)/E10(B₁) that are consequently fully deprotonated. Arg5(A₁), whose side chain is more located in the hydrophobic interface between helix A₁ and B₂, is partially protonated (0.3 – 0.5) and interacts only weakly with the glutamates E9(A₁)/E10(B₂) that are partially protonated. If there is a bulky hydrophobic side chain like Phe or Tyr at position α_5 , the environment of the four glutamates gets more hydrophobic. As a consequence, the sum of protons of these four glutamates rises above unity by about half a proton on average. But, the sum of protons remains below unity with Ala or Leu at position α_5 . In heme conformation (i) the propionates are imbedded in a hydrophobic pocket and consequently fully protonated unless they are involved in salt bridges with Arg at position β_5 , as in structure 6, 17 and 21 where both Arg5(B₁) and Arg5(B₂) form salt bridges with the two propionates. In heme conformation (ii) the propionates are partially solvent exposed and therefore partially deprotonated.

The calculated and measured redox potentials are compared in the correlation diagram, Figure 2. Larger deviations are only observed for the sequences 6, 16, and 21 that contain arginines, but also for the sequences 5 and 11. One reason for these discrepancies is the length of Arg side chain, which makes its



exact position uncertain. Another reason is the protonation state of the arginines, which varies depending on the mutual position with respect to the other titratable groups.

Figure 2. Correlation diagram of measured and calculated redox potentials of 25 different synthetic cyt b. Numbers denote the sequences 1–25 as given below. Open circles refer to heme conformation (i), closed circles to heme orientation (ii) (see text). For the structures of sequences 24 and 25 denoted by + no measured redox potentials are available. The dashed diagonals mark an RMSD of 15mV between measured and computed redox potential. The variable parts of the sequences of helix A and B are denoted as $(\alpha_4 \alpha_5 \alpha_8 \alpha_{12})_A(\beta_4 \beta_5 \beta_8 \beta_{12})_B$. The complete sequence is given in caption of Figure 1. The sequences of the considered synthetic cyt b numbered from 1 to 25 are ordered with falling value of the measured redox potential: (LRALL)_A(QVLL)_B, (AFAAF)_A(QVLL)_B, (AFAAF)_A(QVLL)_B, (AFAAF)_A(QLAL)_B, (LLLLL)_A(QVLL)_B, (LLVLL)_A(QRLA)_B, (VLALL)_A(QVLL)_B, (AFAAF)_A(QLLY)_B, (AFAAF)_A(QAYA)_B, (AFAAF)_A(QLLV)_B, (LLAVL)_A(QAVA)_B, (LLLLL)_A(QAVA)_B, (LLLLL)_A(QLLV)_B, (AYAAY)_A(QLLV)_B, (LRALL)_A(QAYA)_B, (RLALL)_A(QLLV)_B, (LLLLL)_A(QRLA)_B, (FAAFA)_A(QLLV)_B, (LAVLL)_A(QAVA)_B, (ALAAL)_A(QLLV)_B, (ALAAL)_A(QRLL)_B, (LLALL)_A(QAYA)_B, (GLGGL)_A(QAVA)_B, (VLALL)_A(QALA)_B, (ALAAL)_A(QALA)_B.

Exchanging the bulky side chain Phe5(A) by Leu (sequence 2 to 5) the pair of glutamates E9(A)/E10(B) gets more solvent exposed and therefore less protonated. The increase in negative charge in the heme neighborhood leads to a downshift of the redox potential. A general observation is that the redox potential shifts closer to the solution value of –220 mV, if large hydrophobic side chains inside of the heme binding pocket are exchanged by small side chains (sequence 11 to 23). This is due to cavities that are created in the neighborhood of the heme where the dielectric constant is 80.

Analyzing the different synthetic cyt b, we observe shifts of the redox potential by the following mechanisms. At position α_{12} near the propionates and α_8 at the lateral sides of the heme, hydrophobic residues of different size can create cavities inside of the heme binding pocket. Filling these cavities with water shifts the redox potential on the average by 10 mV. The glutamic acids E9(A) and E10(B), at the helix interface (Fig. 1a), are relatively close to the central part of the heme. They are generally negatively charged and yield a downshift of the redox potential by more than 20 mV per Glu. We observe upshifts of the heme redox potential depending on the hydrophobicity, polarity and size of the residues placed at position α_5 that is close to the glutamates E9(A) and E10(B). Bulky hydrophobic

residues like Phe or Tyr at $\alpha 5$ shield the glutamates from the solvent. As a consequence these become partially protonated and contribute to an increase of the heme redox potential by up to 25 mV counteracting the downshift influence of glutamates. In the presence of Arg at $\alpha 4$, $\alpha 5$, $\beta 5$ that can form salt bridges with the acidic groups of propionates, E9(A) or E10(B), these groups remain deprotonated. Nevertheless, the positive charge of the arginines which are closer to the heme than the glutamates yield a shift of the redox potential which is generally upwards varying from -10 to $+35$ mV.

Other mutations at $\alpha 4\alpha 11$ and $\beta 5\beta 12$ are located at the interface between helix pairs A_1/B_1 and A_2/B_2 and refer to hydrophobic residues only. In these cases, the redox potentials are shifted upwards, if the packing of the corresponding side chains is more dense and downward if the packing of the side chains is looser providing place for solvent. Most of the hydrophilic and some of the hydrophobic residues ($\beta 8$ and $\beta 4$) are solvent exposed and distant from the heme. They all have practically no influence on the heme redox potential.

By comparing experimental and computed redox potentials as well as by analyzing the conformational energies of the synthetic cyt b, we found that in the structures 1, 15 and 16 which have arginines at position $\alpha 4$ or $\alpha 5$ close to the open end of the four-helix bundle, the heme is preferentially in conformation (ii) with the propionates oriented toward the open end of the four-helix bundle. For all other structures, better agreement is obtained if the propionates of the heme point toward the template (conformation (i)).

Conclusion

The dependence of the redox potential of the hemes on protein environment was analyzed. Generally, the total shift in the redox potential is mainly due to the low dielectric medium within the protein, bulky hydrophobic residues, the protein backbone charges and the salt bridges formed between arginines and heme propionate groups. The difference in the shift of the redox potentials is due to the interactions with hydrophilic and charged side chains and salt bridges formed with the heme propionates. A detailed discussion of these factors would go beyond the scope of this paper. The present study demonstrates that nowadays methods of modeling and computing of biomolecules can be successfully applied to understand protein-cofactor interactions in atomic detail. It also shows how one can use this ability to design synthetic proteins with desired properties.

Acknowledgments: This work is supported by Ministry of Education, Science and Technological Development of Serbia, research grant 172035. Author is grateful to Prof. Walter Knapp for successful collaboration on the DFG project SFB 498.

Uticaj proteinskog okruženja na osobine kofaktora: Redoks potencijal sintetičkih citohroma b

U ovoj studiji je ispitivan uticaj proteinskog okruženja na pomeranje i fino podešavanje redoks potencijala hema, kao kofaktora, što otvara nove mogućnosti u dizajniranju sintetičkih proteina sa željenim osobinama za različite potrebe, kao na primer biosenzora u bioelektronici i bio-nanotehnologiji. Koristili smo kompjutersko "de novo" modelovanje da bi generisali atomske koordinate 25 sintetičkih proteina strukturno sličnih aktivnom centru citohroma b. Stanje protonovanja titratibilnih amino-kiselinskih ostataka i redoks potencijali hema kao kofaktora u tim proteinima su izračunati na osnovu elektrostatičkih energija, rešavanjem Poason-Bolcmanove jednačine. Rezultati izračunavanja se generalno dobro slažu sa eksperimentalnim merenjima. Analizirali smo zavisnost redoks potencijala hema od razlika u proteinskom okruženju. Generalno, na ukupnu vrednost redoks potencijala utiču niska dielektrična konstanta unutar proteina, veliki hidrofobni ostaci, polarni uticaj amidnih veza osnovnog proteinskog niza i jonski mostovi između propionatnih grupa hema i arginina. Razlike u vrednostima redoks potencijala hema su uzrokovane ovim uticajima. Ova studija pokazuje da se savremene metode modelovanja biomolekula mogu uspešno primeniti kako bi se razumele protein-kofaktor interakcije na atomskom nivou. Takodje je pokazano kako se ovaj pristup može koristiti da bi se dizajnirali sintetički proteini sa željenim osobinama.

References

1. Reviews in *Combinatorial Peptide and Nonpeptide Libraries* (Ed. G. Jung) VCH Weinheim, 1996.
2. a) M. Mutter, S. Vuilleumier, *Angew. Chem. Int. Ed. Engl.* **28** (1989) 535; b) J. W. Bryson, S. F. Betz, H. S. Lu, D. J. Suich, H. X. Zhou, K. T. O'Neil, W. F. DeGrado, *Science* **270** (1995) 935.

3. a) D. E. Robertson, R. S. Farid, C. C. Moser, J-L. Urbauer, S. E. Mulholland, R. Pidikiti, J. D. Lear, A. J. Wand, W. F. DeGrado, P. L. Dutton, *Nature* **368** (1994) 425; b) H. K. Rau, W. Haehnel, *Ber. Bunsen-Ges. Phys. Chem.* **100** (1996) 2052; c) F. Natri, A. Lombardi, G. Morelli, O. Maglio, G. D'Auria, C. Pedone, V. Pavone, *Chem. Eur. J.* **3** (1997) 340; d) S. Sakamoto, I. Obataya, A. Ueno, H. Mihara, *J. Chem. Soc. Perkin Trans. 2* (1999) 2059.
4. a) H. K. Rau, W. Haehnel, *J. Am. Chem. Soc.* **120** (1998) 468; b) E. Katz, V. Heleg-Shabtai, I. Willner, H. K. Rau, W. Haehnel, *Angew. Chem. Int. Ed.* **37** (1998) 3253; c) H. K. Rau, N. De Jonge, W. Haehnel, *Angew. Chem. Int. Ed.* **39** (2000) 250.
5. a) H. K. Rau, N. De Jonge, W. Haehnel, *Proc. Natl. Acad. Sci. USA* **95** (1998) 11526; b) N. De Jonge, H. K. Rau, W. Haehnel, *Z. Phys. Chem.* **213** (1999) 175.
6. a) J. J. Skalicky, B. R. Gibney, F. Rabanal, R. J. Bieber-Urbauer, P. L. Dutton, A. J. Wand, *J. Am. Chem. Soc.* **121** (1999) 4941. b) D. M Popović, S. D Zarić, B. Rabenstein, E. W. Knapp, *J. Am. Chem. Soc.* **123** (2001) 6040. c) G. M. Ullmann, E. W. Knapp, *Eur. Biophys. J.* **28** (1999) 533.
7. a) D. Xia, C. Yu, H. Kim, J. Xia, A. M. Kachurin, L. Zhang, L. Yu, J. Deisenhofer, *Science* **227** (1997) 60; b) S. Iwata, J. W. Lee, K. Okada, J. K. Lee, M. Iwata, B. Rasmussen, T. A. Link, S. Ramaswamy, B. K. Jap, *Science* **281** (1998) 64.
8. B. R. Brooks, R. E. Bruccoleri, B. D. Olafson, D. J. States, S. Swaminathan, M. Karplus, *J. Comp. Chem.* **4** (1983) 187.